High Temperature, Vol. 39, No. 2, 2001, pp. 169–179. Translated from Teplofizika Vysokikh Temperatur, Vol. 39, No. 2, 2001, pp. 187–197.

PLASMA INVESTIGATIONS

Reverse-Flow Swirl Radio-Frequency Induction Plasmatron

A. F. Gutsol[1], J. Larjo[2], and R. Hernberg[2]

[1] *Institute of Chemistry and Technology of Rare Elements and Minerals, Kol'skii Scientific Center, Russian Academy of Sciences, Apatity, Murmansk oblast, 184200 Russia*

[2] *Tampere University of Technology, P.O. Box 692, FIN-33101, Tampere, Finland*

Received February 9, 2000

Abstract—Experimentally observed modes of an rf induction (RFI) discharge in argon with reverse-flow swirl stabilization are described. The data on the simulation of RFI plasmatrons are analyzed; it is demonstrated that, for the case of highly swirling flows, a correct inclusion of gasdynamic effects is of most importance. The procedure employed for simulation was previously used in a direct-flow swirl plasmatron with nondiaphragmed outlet to demonstrate that an intense swirling of flow results in the emergence of reverse flow over the entire length of the plasmatron chamber. The direct-flow swirl and reverse-flow swirl stabilization methods are compared from the standpoint of efficiency of plasma jet generation with the aid of calorimetric measurements and numerical simulation of an argon RFI plasmatron of constant geometry. It is demonstrated that the reverse-flow swirl stabilization is more efficient from the standpoint of possible applications of RFI discharge.

INTRODUCTION

Radio-frequency induction (RFI) plasmatrons, first described by Reed [1, 2], have found extensive application, first of all, in the field of high-temperature treatment of materials. They compare favorably with arc plasmatrons thanks to the relatively low velocity and large volume of plasma and, what is more important, the absence of electrodes, which provides for a high purity of plasma. As compared with ultrahigh-frequency (UHF) plasmatrons, RFI plasmatrons are also characterized by some advantages such as the relative simplicity and availability of supply sources of different power and frequency, as well as a higher enthalpy of plasma. The recently suggested method of reverse-flow swirl stabilization (RSS) and heat insulation [3] was tested in application with a UHF plasmatron and gas combustor [4], whereby their performance was improved sharply. The prospects for applying this method to RFI plasmatrons as well appeared quite promising. In this paper, we treat the results of preliminary investigation of a reverse-flow RFI plasmatron, describe the experimentally observed modes of RFI discharge in argon with RSS, and compare the direct-flow swirl and reverse-flow swirl methods of stabilization from the standpoint of efficiency of plasma jet generation with the aid of calorimetric measurements and numerical simulation of an argon RFI plasmatron of constant geometry.

PRELIMINARY EXPERIMENTAL STUDY OF REVERSE-FLOW RFI PLASMATRON

A fundamental difference exists between an RFI plasmatron and objects used previously to test the RSS principle (microwave discharge, gas flame [3, 4]). The recirculation flow in ordinary swirl flows provides for stabilization of plasma and flame owing to the transfer of active particles, i.e., radicals, ions, and electrons, downstream. In so doing, it is the central hot zone in the flame and microwave discharge, in which the energy release occurs, that is the source of those active particles. In the RFI discharge, the absorption of energy occurs in the toroidal skin layer *8* (Fig. 1) whose diameter defines the efficiency of absorption of the rf energy. In the case of RSS, a flow directed toward the axis *a priori* exists in the entire skin volume; along with the Lorentz force, this flow must bring about a reduction in the diameter of the zone of energy release and, consequently, decrease the efficiency of the inductor-plasma electromagnetic coupling. In addition, with such a stabilization, a plasmoid may be free of recirculation "stagnation" zones which usually represent the sources of active particles. Therefore, the stability of an RFI plasma with RSS must be lower than that of a plasma with direct-flow swirl stabilization (DSS) and lower than the stability of a UHF plasma and gas flame with RSS.

Preliminary experiments in the stabilization of an RFI discharge in a reverse swirl flow of argon were per-

0018-151X/01/3902-0169$25.00

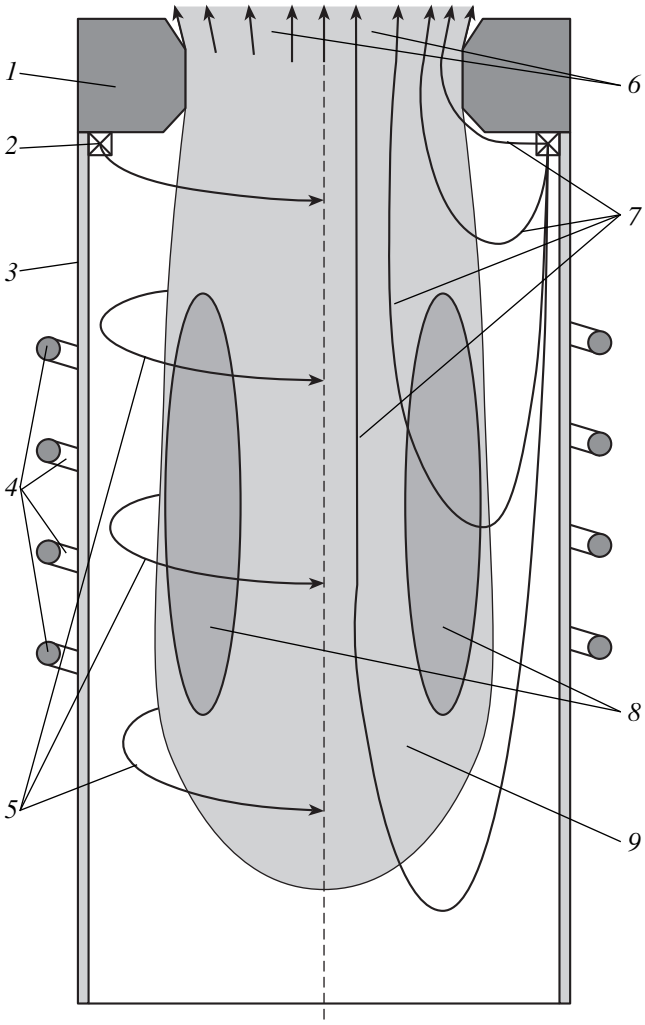

Fig. 1. Schematic of an RFI plasmatron with reverse-flow swirl stabilization: (*1*) water-cooled nozzle, (*2*) tangential swirler of plasma-forming gas, (*3*) quartz pipe, (*4*) inductor, (*5*) lines of travel of plasma-forming gas, (*6*) outgoing jet of plasma, (*7*) assumed lines of travel of gas and plasma in the axial plane, (*8*) toroidal skin layer, (*9*) plasma.

formed using an 11-60/1.76 RFI generator retuned to the frequency of 2 MHz. The plasmatron quartz pipe *3* (Fig. 1) with an inside diameter of 75 mm and outside diameter of 80 mm was cooled on the outside by an axial flow of air. A four-turn inductor *4* had a length of 100 mm and an inside diameter of 90 mm. The distance between the plane of nozzle *1* facing the discharge and the inductor was 70 mm. The diameter of the flow area of the nozzle installed in the top portion of the vertically arranged plasmatron was 50 mm. Argon was delivered tangentially in the vicinity of the nozzle via four holes 2 mm in diameter located on a radius of 36 mm. In some experiments, nitrogen was admixed to argon.

Depending on the pressure, gas flow rate, and generator power, several modes of discharge could be identified, with differences between them observed visually.

1. The pressure $P \simeq 10$ kPa, the generator power $W =$ 9.5 kW, and the flow rate of argon $Q = 0.45$ to 0.65 g/s (Fig. 2a). The discharge has an unusual shape of a droplet or inverted mushroom. The "thickest" rose-colored part of such a discharge, located inside the inductor, may have a diameter equal to the inside diameter of the quartz pipe. The diameter of the "thin" yellow part directed toward the nozzle is approximately 40 mm.

2. The pressure $P \simeq 35$ kPa, the generator power $W = 25$ kW, and the flow rate of argon $Q = 0.75$ g/s (Fig. 2b). This is an interesting mode with a very large specific energy contribution $J = W_d/Q$, where W_d is the power absorbed by the discharge. The bright white zone of the discharge has a conic shape with a base 57 mm in diameter at the level of the lower turn of the inductor. The narrow part of the cone 20 mm in diameter is directed toward the nozzle. The bright white cone is surrounded by a zone of rose-colored glow 45 mm in diameter at the nozzle level.

3. The pressure $P \simeq 50$ kPa, the generator power $W = 8$ to 9 kW, and the flow rate of argon $Q = 0.5$ g/s. This is an unstable mode. The discharge is cigar-shaped, with the maximum diameter of 42 mm inside the inductor.

4. The pressure $P \simeq 50$ kPa, the generator power $W = 9.5$ to 13 kW, and the flow rate of argon $Q = 0.8$ to 1.2 g/s (Fig. 2c). The discharge is shaped as a combination of two cones. The narrow part of the top cone is located in the neighborhood of the nozzle and has a diameter of about 50 mm, which corresponds to the nozzle diameter. The vertex of the second cone goes somewhat beyond the inductor limits. Both cones have a common base 60 to 65 mm in diameter in the neighborhood of the middle of the inductor.

5. The pressure $P \simeq 50$ kPa, the generator power $W = 16$ to 22 kW, and the flow rate of argon $Q = 1.3$ to 3.3 g/s (Fig. 2d). The barrel-shaped discharge is very stable. The base of this "barrel" 62–70 mm in diameter is located somewhat below the last (bottom) turn of the inductor, and its top portion 55 mm in diameter touches the nozzle. One can distinguish the dark flow core in the vicinity of the nozzle. An atmospheric-pressure discharge with $W = 25$–36 kW and $Q \geq 1.8$ g/s is of approximately the same shape. In the case of the generator power $W = 13$ to 18.5 kW and the flow rate of argon $1.8 \text{ g/s} > Q \geq 0.9$ g/s, an atmospheric-pressure discharge develops a plasma "tail" going far beyond the inductor limits (this is probably due to the axial downward flow). Apparently because of the flow rotation, the plasma of atmospheric-pressure discharge flows out of the discharge chamber only on the periphery of the nozzle.

Experiments were performed involving the introduction of an additional axial flow from the chamber

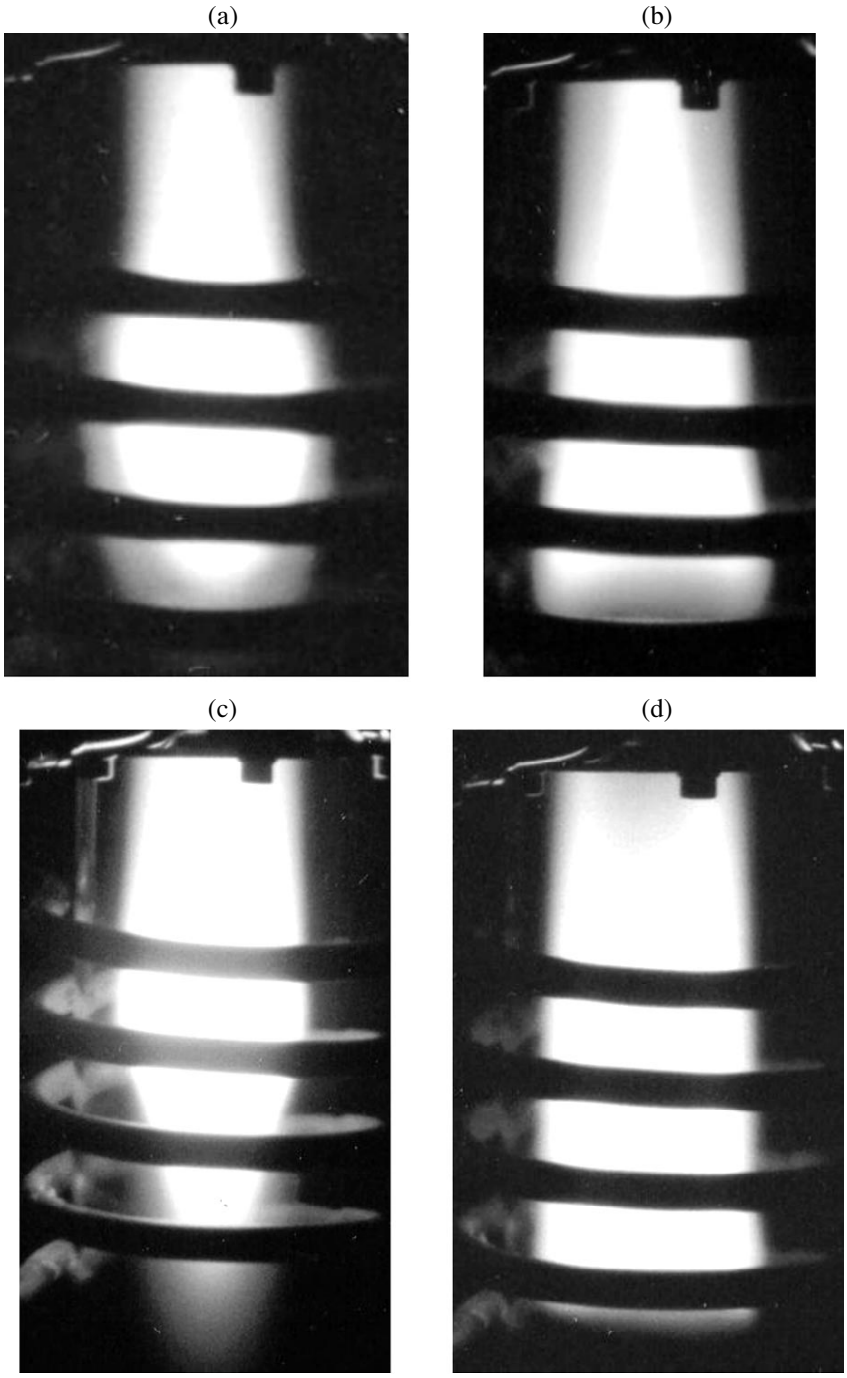

Fig. 2. An RFI discharge with RSS for different values of W, P, and Q: (a) $P \simeq 10$ kPa, $W = 9.5$ kW, $Q = 0.45$–0.65 g/s; (b) $P \simeq 35$ kPa, $W = 25$ kW, $Q = 0.75$ g/s; (c) $P \simeq 50$ kPa, $W = 9.5$–13 kW, $Q = 0.8$–1.2 g/s; (d) $P \simeq 50$ kPa, $W = 16$–22 kW, $Q = 1.3$–3.3 g/s.

bottom to an atmospheric pressure RFI discharge with RSS. The gas was delivered from a pipe with an inside diameter of 4.5 mm, whose outlet hole was located 60 mm below the inductor. While this additional flow was weak, a certain instability of discharge burning was observed; this was apparently due to a collision between the downward axial flow from the plasma and the additional flow. As the additional axial flow increased, the discharge stabilized, and the gas flow rate in the additional flow could reach the same value as that in the main swirl flow. In the mode with additional axial flow, the plasma jet issued from the plasmatron in the vicinity of the nozzle axis. Nitrogen could be admixed to the additional axial flow. In this case, the

discharge diameter decreased, and the generator power had to be increased to maintain the discharge.

Therefore, the preliminary study has demonstrated that an RFI discharge may be stabilized with the aid of a reverse swirl flow of argon. In so doing, in all modes of the discharge, the issuing plasma jet continued to glow (which points to its very high temperature), at least, up to the water-cooled nozzle. In addition, a comparison of the obtained results with the available experience of operation with a direct-flow swirl RFI plasmatron leads one to conclude that a reverse-flow swirl RFI plasmatron is capable of operating with greater specific energy contributions than a direct-flow swirl plasmatron with the same intensity of cooling. This is indicative of a better hydrodynamic isolation of plasma from the wall. Of considerable engineering interest is the stability of an RFI plasma with RSS with respect to axial flow which may transport a material intended for high-temperature treatment.

In studying reverse-flow swirl RFI discharges, we came across a little-cited publication by Reed [5], in which he reported the use of RSS of an RFI plasma in one of his spectroscopic experiments. Because Reed placed his entire plasmatron in a container with water for cooling and failed to make any comments concerning the employed method of stabilization, it remains unclear whether he could estimate the other advantages of the method in addition to the possibility of extracting the radiation on the side of the closed end of the plasmatron.

ANALYSIS OF THE DATA ON SIMULATION OF RFI PLASMATRONS

RFI plasmatrons are popular as an object for physical and numerical simulation. A review of early papers dealing with the simulation of RFI plasma was made by Dresvin [6]. The gasdynamic and electrodynamic processes in an RFI discharge are interrelated; indeed, considerable progress in describing the motion of RFI plasma was made by Boulos [7], who performed numerical simulation of RFI plasma using a self-consistent model incorporating the equations of both electrodynamics and gas dynamics, with due regard for thermal conductivity and radiation loss. A discharge stabilized by direct wall flow was simulated (for more detail about various schemes of stabilization of RFI discharges, see [8]). The flow of gas was assumed to be laminar, and a one-dimensional description of the electromagnetic field was used. The axial velocity profile on the inlet to the plasmatron was taken to be smooth with a flat central portion. With rare exception, the same stabilization scheme was treated in all other studies associated with the simulation of RFI plasma.

Following the publications [9, 10], the simulation was usually performed with due regard for the two-dimensionality of the electromagnetic field. Sometimes, it is very important, for example, when a metal pipe for the injection of reagents is introduced into the inductor zone [11], or when one attempts to include the inductor shape [9]; however, as a rule, the transition to the two-dimensional model of electromagnetic field changes little the predicted pattern of flow and temperature field [10]. Because the gas viscosity increases with temperature and the density decreases, it is usually assumed that the flow in the plasmatron is laminar. Nevertheless, attempts were made to include turbulence using both the standard k–ε model [12–14] and its modifications [15–17]. There is no fundamental difference between the flow patterns obtained on the assumption of laminarity and in view of turbulence. A recirculation zone always exists in the upstream portion of the inductor. A developed turbulence is observed in the wall layer and at the point of collision between the flow of plasma-forming gas and the recirculation zone. In almost all studies, a comparison is made with the results of other model calculations rather than with experimental data. This is due to the complexity of experimental investigation of the velocity field, especially, in the hot zone of the discharge [18]. Therefore, the significance of most studies into the simulation of RFI plasma is in the inclusion of an ever larger number of possible effects such as the deviation from local thermodynamic equilibrium (LTE) [19]. Under atmospheric pressure, the condition of LTE is valid with good accuracy for the bulk of RFI plasma. The maximum temperature of the discharge T_{max} is a very conservative characteristic, which mainly depends on the type of gas [6].

The cases of rotation of gas in a plasmatron are treated rather seldom. Chen and Boulos [13] used the k–ε model of turbulence to simulate a three-flow RFI plasmatron (high-velocity direct wall flow, low-velocity intermediate, and narrow central flows). Imparting rotation at a speed of 10 m/s to the intermediate flow, which amounted to only 1/8 of the total gas flow rate, caused a sharp variation of the resultant pattern: the plasma extended upstream, T_{max} decreased, and the center of the recirculation zone found itself outside of the limits of plasma formation.

We failed to find publications describing the simulation of RFI plasma in a highly swirling flow, with the gas delivered to the plasmatron tangentially at a high rate. It is by gas dynamics that the main effects are defined, and an increase in the rate of delivery and flow of gas may cause a halving of the discharge diameter, from 0.8 to 0.4 of the pipe diameter [20]. We will make a comparison of the forces detaching the plasma away from the pipe wall, i.e., the Lorentz force and Archimedes' force which makes the plasma "float up" in the field of centrifugal forces. The experimental and prediction data on the maximum value of electromagnetic force in [11, 21–23] give values in the range of 300 to 1000 N/m^3. The value of 3×10^{10} N/m^3 [10] must apparently be regarded as an error on the graph

axis. Archimedes' force

$$F_a = (\rho_g - \rho_p)w^2/R \quad (1)$$

may be evaluated by substituting the characteristic values of density $\rho_g = 1.8$ kg/m^3 for argon, circumferential velocity of flow $w = 30$ m/s, and pipe radius $R = 0.03$ m. The plasma density $\rho_p \ll \rho_g$. Estimates show that Archimedes' force exceeds the force of electromagnetic compression of plasma by more than an order of magnitude. Therefore, in simulating RFI plasma with swirl stabilization, special attention must be given to gas dynamics. The estimation of the values of the Reynolds number indicates that the gas flow must be turbulent even in the tangential delivery channels and, the more so, after the gas is delivered to the plasmatron pipe. A high temperature may suppress the turbulence inside a plasmoid; however, the velocity of flows past the plasma will be defined primarily by the turbulent deceleration because of the pipe walls. Therefore, it is of fundamental importance to include the turbulence in the case of swirl stabilization; it is known from the experience in computational gas dynamics and simulation of swirl flows [24] that, in this case, it would be incorrect to use the standard k–ε model of turbulence.

As a result of comprehensive analysis of the problem of simulation of RFI plasma with swirl stabilization, it was decided to use the method that was already tested in simulating UHF plasma [4]. The flow and heat transfer were calculated using the FLUENT commercially available dedicated computer codes, and the absorption of electromagnetic energy by plasma was simulated using the zone of heat release. Because it is impossible to explicitly include the electromagnetic interaction in the FLUENT software, one had to make sure of the adequacy of such simulation using a well-studied example. Such an example was provided by the conditions of the experiment performed previously [25] in an RFI plasmatron with DSS and nondiaphragmed outlet, which was destined for updating. The results of this test simulation are described in [26]. Below, we will describe the approach employed, which was also used in this study, as well as the main results and conclusions.

In view of the experimental data of [25] (the maximum electron concentration of 1.1×10^{22} m^{-3}, which, on the assumption of local thermodynamic equilibrium, corresponds to the temperature of 9500 K), the generator frequency of 2 MHz, and the prediction data of other researchers [10, 11, 27], the total thickness of the layer of heat release was taken to be 18 mm. After studying the photographs of the discharge, it was agreed that the heating of plasma occurred in a circular zone 120 mm long (the inductor length, 100 mm). By estimating the average conductivity in the zone of heat release (by the discharge temperature) $\sigma \simeq 1500$ Ohm^{-1} m^{-1}, the zone volume V, and the power $W_d = 14$ kW absorbed by the discharge, we could estimate the density of current j in this zone, $j^2V/\sigma = W_d$. In view of the experimental data about the value of current in the inductor, we could estimate the force of magnetic pressure compressing the plasma, which was included by preassigning the sources of the force directed toward the axis in the same cells in which the value of heat release was preassigned, with the force being proportional to heat release. The cases of uniform and nonuniform energy release within the circular zone were treated. The data on the heat capacity, viscosity, and thermal conductivity of plasma [6] were interpolated in the form of piecewise linear functions.

In order to include radiation heat transfer, use was made of the model of discrete radiation transfer included in the FLUENT computer codes. In so doing, one had to introduce for plasma the dependence of the absorption coefficient a on the temperature T. The absorption coefficient is related to emissivity (blackbody radiation model). The necessary data of [28] were approximated by the formula

$$\log a = -0.18 - 0.85[(15 - 10^{-3}T)/4.5]^{2.32}. \quad (2)$$

Because $a \ll 1$ in the entire range, we treat the plasma in this model as optically thin (as most other authors do).

The simulation with the aid of the FLUENT computer codes (version 4.47) was performed in axisymmetric geometry (two-dimensional model with due regard for tangential velocity). The turbulence was calculated using the Reynolds stress model in combination with the nonequilibrium "wall" function and inclusion of the directional diffusion of turbulence. A fairly reasonable temperature field with $T_{max} = 9062$ K and reverse flow extending over the entire length of the discharge chamber were obtained for a nondiaphragmed plasmatron with DSS. The simulation result varied insignificantly upon doubling of the number of mesh points, as well as when a uniform heating zone was used or the electromagnetic compression of plasma was ignored.

The reverse flow over the entire length of the chamber is not a necessary result for DSS. In the calculation performed for half the pressure (50 kPa) with the values of initial velocity unchanged, the recirculation zone extended only to the middle of the inductor, but the level of T_{max} changed little. If the gas velocity at the inlet increases simultaneously with and proportionally to the decrease in pressure (the condition of unchanged flow rate with invariable area of the inlet holes), the pattern of fields of flow and temperature remains almost unvaried. This is due to the fact that the formation (and, accordingly, destruction) of recirculation zones in direct swirl flows depends on the swirl number of flow S [29],

$$S = (\int r^2 wu dr)/(R_0 \int ru^2 dr). \quad (3)$$

Here, w and u denote the tangential and axial velocity, respectively; r is the integration radius; and R_0 is the maximum radius in this cross section of the channel. The reduction of the pressure at the inlet by half with the tangential velocity unvaried leads to a reduction of the swirl number approximately by half. A proportional increase of all components of velocity maintains the swirl number unvaried. In our case, $S \simeq 8$.

The results of simulation of a direct-flow RFI plasmatron with DSS has demonstrated [26] that a correct inclusion of turbulence for swirl flows is more important than the inclusion of nonuniformity of energy release and electromagnetic forces. In fact, in order to calculate with reasonable accuracy the temperature and flow fields in swirl plasmatrons, one must know the approximate location and shape of the zone of energy release (this information may be obtained from photographs of the discharge), the total released power (exact data may be obtained by calorimetric measurements, and the estimates, from the power of the generator and the diameter of the plasma formation), as well as the internal geometry of the chamber and incoming gas flows. The correlation between the electromagnetic and gasdynamic components of the problem proved to be insignificant.

CALORIMETRIC MEASUREMENTS AND NUMERICAL SIMULATION OF REVERSE-FLOW SWIRL AND DIRECT-FLOW SWIRL RFI PLASMATRONS

In order to characterize the relative efficiency of the developed plasmatron with RSS and of a plasmatron of the same geometry with DSS as plasma jet generators, we performed their complete calorimetric measurements at atmospheric pressure in argon and appropriate numerical simulation. For calorimetric studies, the quartz pipe of the plasmatron was subjected to film water cooling (which was probably analogous to that used by Chen and Boulos [12]), and a water-cooled heat exchanger was joined to the nozzle. The distance between the inductor center and the nozzle was 130 mm. The quartz pipe was 380 mm long. The plasmatron could function in both the RSS (Fig. 1) and the DSS modes. In the latter case, argon was delivered via six square tangential holes with a side of 2 mm, located at the chamber bottom on a radius of 38 mm.

The calorimetric measurements included the measurements of the temperature and the flow rate of water used to cool the quartz pipe, nozzle, and heat exchanger (separately), as well as of the water temperature at the inlet. The water flow rate was measured by KROHNE VA 20 rotameters, and the temperature measurements were performed by shielded thermocouples, with the results read out automatically using an SR630 16-channel interface (manufactured by Stanford Research Systems, Inc.) and printed out every twelve seconds. The gas temperature after the heat exchanger was monitored analogously, but this temperature at all times was low enough not to take into account the energy removed by gas. The radiation energy flux was measured at a distance of 1.3 m from the plasmatron by a surface detector absorbing as a blackbody and employed for standard measurements of radiated laser power. This flux was integrated with respect to solid angle in view of the fact that a part of radiation was absorbed by the cooled components of the plasmatron. The sum of measured energy fluxes (nozzle, quartz pipe, heat exchanger, and radiation) was equal to the power W_d absorbed by the discharge from the inductor. This power was measured within ~3% and amounted to 55–75% of the generator power, depending on the mode of operation.

The results of experiments in a discharge with DSS and diaphragmed outlet demonstrated an extremely high stability of this discharge. Without varying the argon flow rate Q_{Ar}, one could vary the generator power W_0 by an order of magnitude: for example, with Q_{Ar} = 1.4 g/s, W_0 was varied from 4 to 49 kW. The discharge remained stable, and only its brightness and volume varied. The W_d/W_0 ratio for all modes was approximately 64%. The reason for this high stability of the discharge is clear from the simulation results (Fig. 3a). The main flow of gas moves past the discharge and cools it only on the surface. The discharge "lives its own life," with the amount of gas pumped through the discharge with the aid of electromagnetic forces being the larger, the higher the power.

The energy characteristics of a discharge with DSS, such as the dependence of the mean enthalpy j_p of the plasma jet on the generator power W_0 (Fig. 4) and the dependence of the plasmatron efficiency η on the power W_d absorbed in the discharge (Fig. 5), are fairly typical. By the plasmatron efficiency η is meant the ratio of power in a plasma jet W_p (in our case, it is equal to the power released in the heat exchanger) to the total power W_d absorbed by the discharge, $\eta = W_p/W_d$. An increase in W_0 with a constant flow rate of argon Q_{Ar} leads to an increase in the jet enthalpy j_p, but only to a level of 3 kJ/g. An increase in Q_{Ar} with a constant value of W_0 leads to a decrease in j_p (Fig. 4). The efficiency η drops with an increase in W_d and with a decrease in Q_{Ar} (Fig. 5). Therefore, an RFI discharge with DSS enables one to obtain a high-enthalpy jet in the case of a low efficiency or a low-enthalpy jet in the case of a relatively high efficiency. One can see (Fig. 5) that the experimental results and the results of numerical simulation are in reasonable agreement with each other.

As to the stability of a discharge with RSS, its energy threshold of existence is much higher than in the case of an RFI discharge with DSS. The minimal value of W_0 for RSS is at a level of 15 kW with Q_{Ar} = (1.4–2.3) g/s. The plasmatron efficiency (Fig. 6) for an RFI discharge with RSS likewise decreases with an increase in W_d and a decrease in Q_{Ar}, though reaching a higher value than in the case with DSS. An RFI plas-

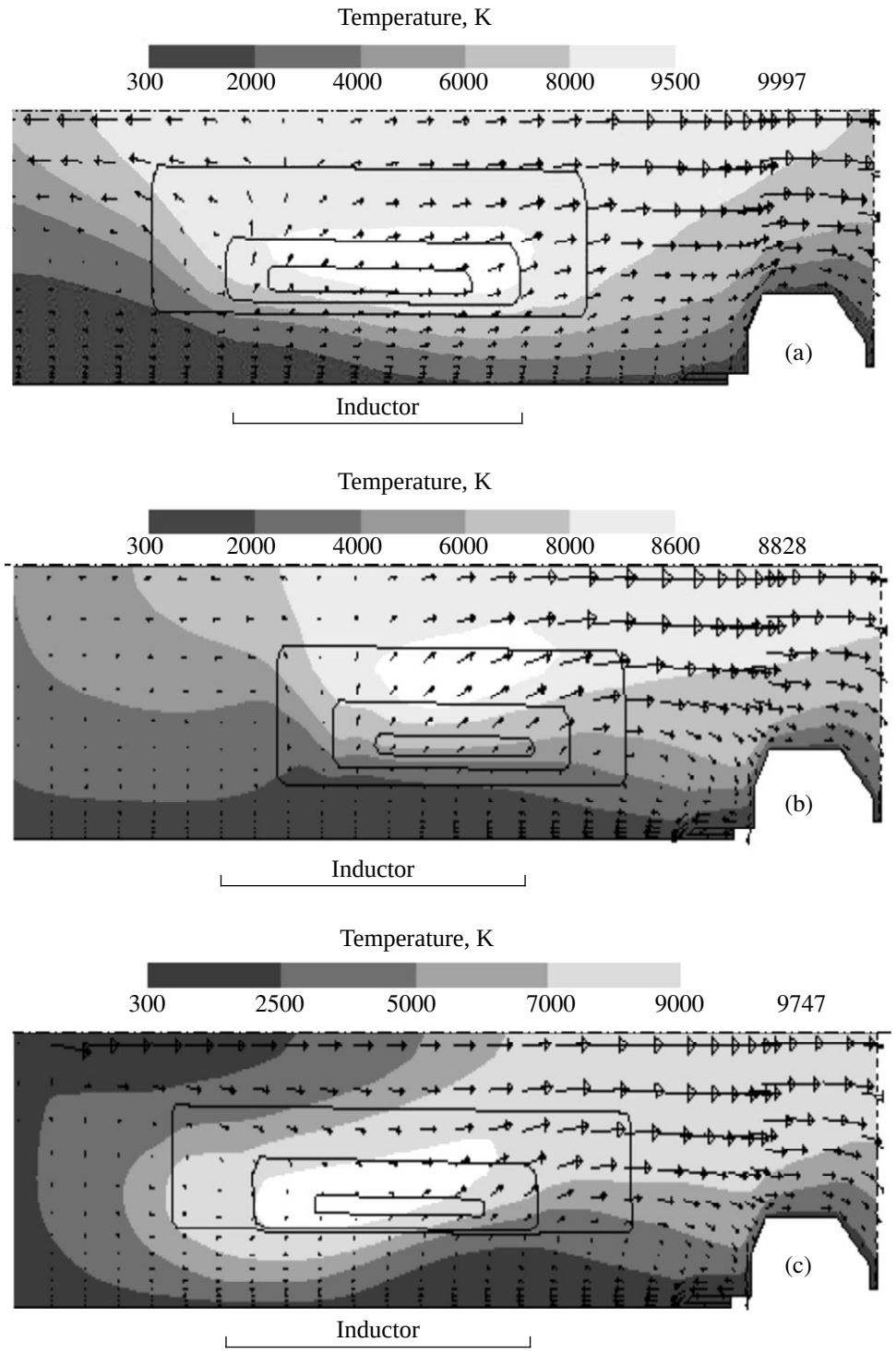

Fig. 3. The results of simulation of RFI plasmatrons with nozzle: (a) DSS—W_0 = 17 kW, Q_{Ar} = 1.4 g/s; (b) RSS—W_0 = 14 kW, Q_{Ar} = 2.1 g/s; (c) RSS—W_0 = 21 kW, Q_{Ar} = 2.1 g/s + 0.7 g/s (in axial flow). Gray shades indicate the temperature fields; arrows indicate the velocity vectors in the axial plane; closed curves indicate the contours of the heating zones and of the negative radial moment of Lorentz force—the largest zone: (a) 3×10^7 W/m^3 and 120 N/m^3, (b) 2.58×10^7 W/m^3 and 100 N/m^3, (c) 3.68×10^7 W/m^3 and 150 N/m^3; the intermediate zone: (a) 9×10^7 W/m^3 and 360 N/m^3, (b) 7.75×10^7 W/m^3 and 300 N/m^3, (c) 11×10^7 W/m^3 and 450 N/m^3; the smallest zone: (a) 13.5×10^7 W/m^3 and 540 N/m^3, (b) 11.6×10^7 W/m^3 and 450 N/m^3, (c) 16.5×10^7 W/m^3 and 675 N/m^3.

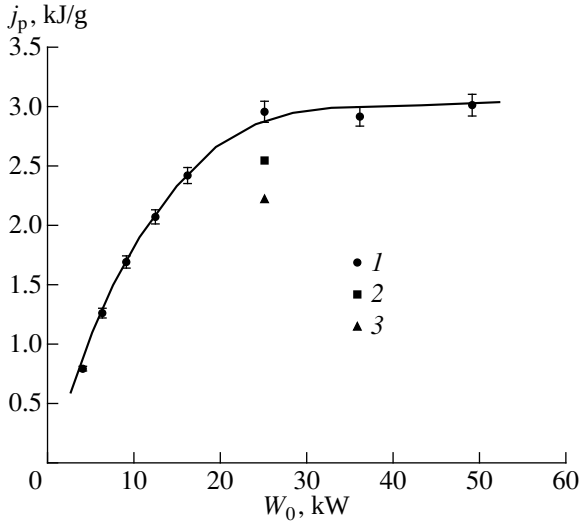

Fig. 4. The experimentally obtained dependence of j_p on W_0 for a discharge with DSS. The flow rate of argon: (*1*) 1.4, (*2*) 2.3, (*3*) 3.2 g/s.

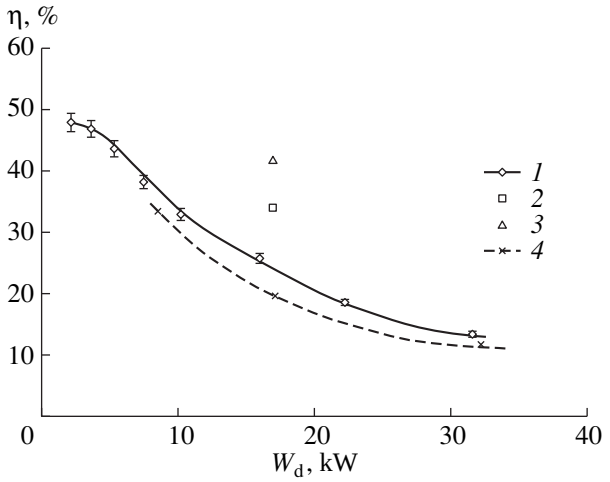

Fig. 5. The experimentally obtained (*1–3*) and predicted (*4*) dependence of η on W_d for a discharge with DSS. The flow rate of argon: (*1*, *4*) 1.4, (*2*) 2.3, (*3*) 3.2 g/s.

matron with RSS reaches the maximum value of η with a constant value of W_0 at the limit of stability with increasing flow rate of gas. In so doing, the discharge increases in size appreciably and even fails to reach the bottom turn of the inductor (Fig. 7). The enthalpy of the jet generated by an RFI discharge with RSS is in all instances higher than 2 kJ/g and increases both with increasing W_0 and with increasing Q_{Ar} (Fig. 8), this being highly unusual for any type of discharge. The reason for this may be understood after analyzing the results of numerical simulation (Fig. 3b). In addition to the main reverse swirl flow, the electromagnetic forces cause the emergence of an additional recirculation flow in the vicinity of the closed end of the plasmatron. It is this additional recirculation that is apparently responsible for the formation of a plasma "tail" observed in some modes during preliminary investigation and leads to an increase in the plasma volume, to additional heat removal to the plasmatron wall, and to radiation loss. Note that the fraction of radiation loss in the overall energy balance of an argon RFI plasmatron with RSS varied in a wide range from 8 to 32%. The enthalpy of the main flow passing through the zone of energy release must be high and approximately constant, because it is defined directly by the discharge temperature. An increase in Q_{Ar} leads to a compression of the plasma formation, to a decrease or suppression of the secondary recirculation zone, and, consequently, to a decrease in the plasma volume, i.e., to a decrease in the energy loss. This reduction of energy loss proves to be so appreciable as to bring about a rise of j_p. This unusual property of RFI discharge with RSS makes it a very attractive tool for generation of high-enthalpy jets. The fraction of power absorbed by the discharge from the generator, W_d/W_0, increases with the plasma volume and varies within 55–66%. One can see (Fig. 6) that the model calculation results enable one to predict with good accuracy the efficiency of an RFI plasmatron with RSS. A significant disagreement between the experimentally obtained curve and the calculation result is observed only outside of the range of stable burning of the discharge (see the data for Q_{Ar} = 3.21 g/s and W_d = 14 kW). The resultant, very high, efficiency is especially important for systems in which the nozzle is a

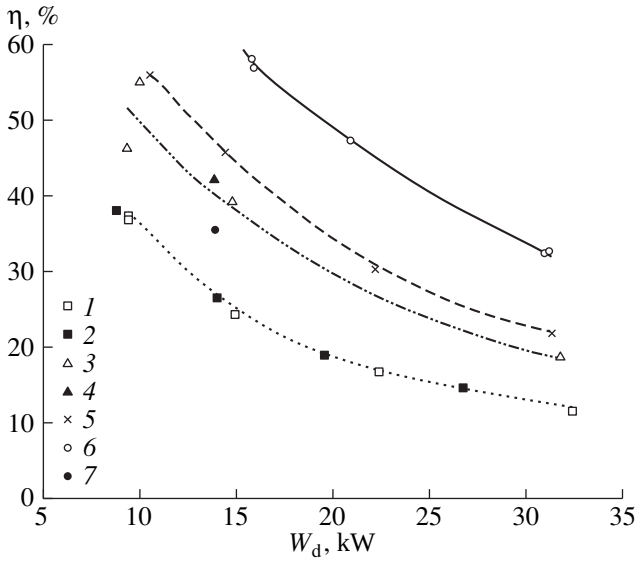

Fig. 6. The experimentally obtained (*1*, *3*, *5*, *6*) and predicted (*2*, *4*, *7*) dependence of η on W_d for a discharge with RSS. The flow rate of argon: (*1*, *2*) 1.4, (*3*, *4*) 2.1, (*5*) 2.3, (*6*, *7*) 3.2 g/s.

structural component of fundamental importance, for example, in sources of supersonic plasma jets [31].

According to the simulation results (Fig. 3b), some recirculation is also observed in the vicinity of the swirler: this recirculation must bring about an intense heat flux to the nozzle surface. This result contradicts our notions of flows in such systems [31], according to which a flow directed toward the center and protecting the nozzle surface against overheating must exist in the vicinity of the nozzle surface. Indeed, the measured heat loss in the nozzle (6 to 16%) proved to be approximately twice less than the predicted values. The reason for this disagreement is probably due to the inadequately fine computational mesh in the vicinity of the nozzle surface. Unfortunately, a further finer division of the mesh resulted in a sharp increase in the time required for computations. (The nonuniform and nonrectangular computational mesh contained 226×30 cells. The calculation region included only the inner space of the plasmatron. A time of several hours was required for calculation of a single mode in an Alpha Station 600 5/333.)

One can see the advantages of RSS over DSS in Fig. 9, where the data are given for a low-flow-rate mode (Q_{Ar} of about 0.5 g/s with W_0 = 16 kW, j_p = 3.2 to 3.4 kJ/g, and η of about 15%). In spite of the relatively low efficiency, this mode may be of interest from the standpoint of sources of high-enthalpy plasma in instruments for spectral chemical analysis, when a low flow rate of argon is of fundamental importance.

It is possible that the property of RFI discharge with RSS of most practical importance is its stable burning under conditions of intense additional axial delivery of gas (the results of simulation in Fig. 3c). One can see that the additional flow causes little distortion of the initial flow pattern. Calorimetric measurements in such a mode produced the following data: with W_0 = 49 kW, a flow rate Q_{Ar} = 2.29 g/s through the swirler, and an additional axial flow of nitrogen of 0.85 g/s, the power W_d absorbed by the discharge amounted to 36.46 kW (74.4% of W_0) with η = 48.4% and j_p = 5.62 kJ/g, which corresponds to a temperature of approximately 6000 K for the given mixture of argon and nitrogen. A stable burning of the discharge with an intense additional axial flux provides for the possibility of injecting reagents (both gaseous and disperse) into the active zone of the discharge. In so doing, according to the existing notions, the products of interaction must not actively interact with the plasmatron wall. It is the absence of such properties in conventional RFI discharges that restricts sharply the scope of their applications in plasma chemistry (see, for example, [11]). It is not quite clear to what extent the flow rotation will promote the ejection from the high-temperature zone of the disperse phase introduced with the additional flow. The radial migration of turbulent elements which are decelerated at the cylindrical wall [31] must bring about the formation, at the center of flow, of a region with a low rate of rotation. In flows with intense rotation, some researchers observed experimentally [32, 33] such regions which almost did not rotate or rotated in the opposite direction. At any rate, the results of a test

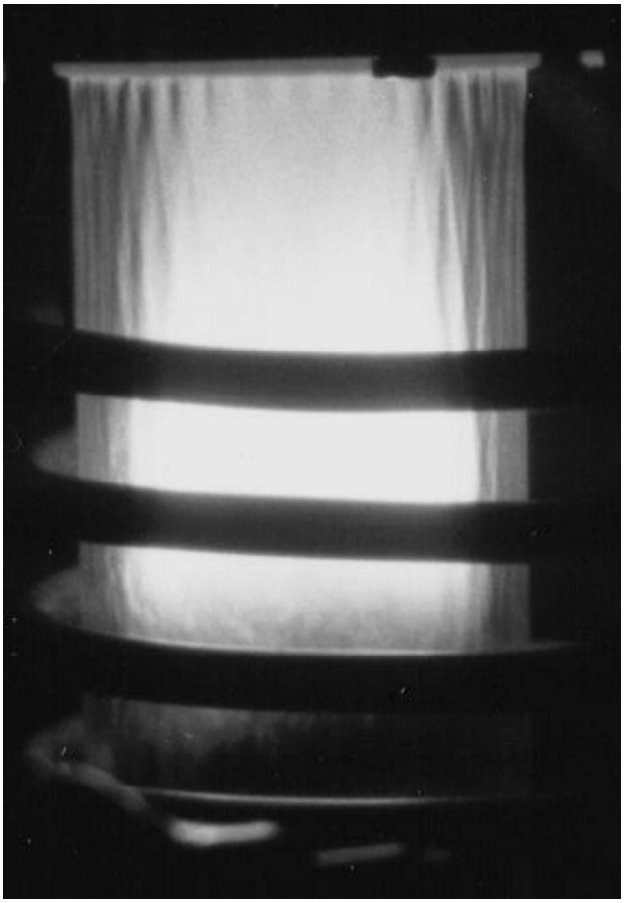

Fig. 7. A discharge with RSS: W_0 = 16 kW, Q_{Ar} = 2.1 g/s.

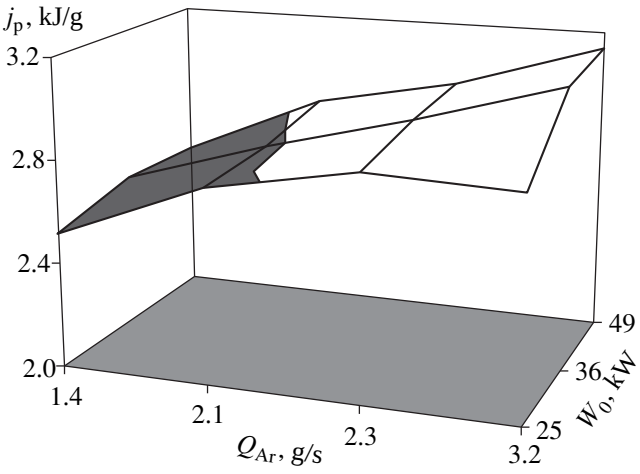

Fig. 8. The experimentally obtained dependence of j_p on W_0 and Q_{Ar} for a discharge with RSS.

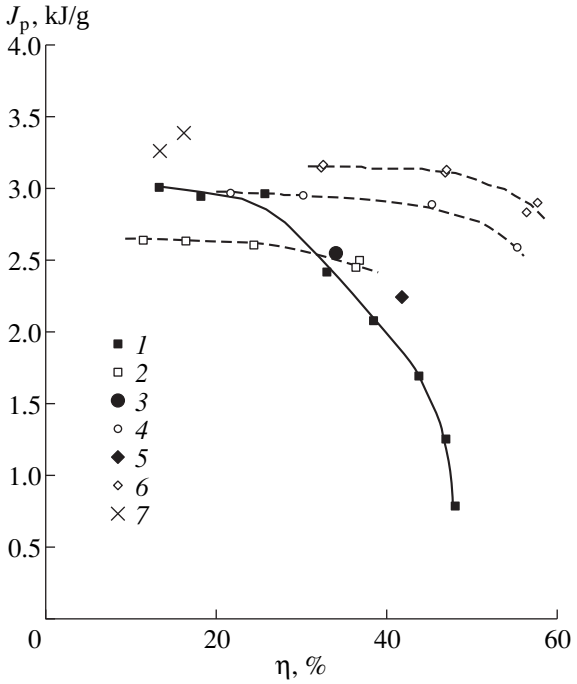

Fig. 9. The correlation between j_p and η for plasmatrons with DSS (*1*, *3*, *5*) and RSS (*2*, *4*, *6*, *7*) for different values of Q_{Ar}: (*1*, *2*) 1.4, (*3*, *4*) 2.29, (*5*, *6*) 3.21, (*7*) 0.5 g/s.

experiment with axial injection of zirconia powder into a microwave discharge of 3.5 kW with RSS demonstrated the variation of the particle shape to spherical with a diameter of up to 100 μm [4], which indicated that the particles passed through the zone of energy release.

As has been demonstrated by the results of our study, an RFI discharge with RSS may find a more extensive application than conventional RFI discharges.

ACKNOWLEDGMENTS

This study received financial support from the Russian Foundation for Basic Research (grant no. 98-01-00021) and from the Finnish Academy of Sciences.

REFERENCES

1. Reed, T.B., *J. Appl. Phys.*, 1961, vol. 32, no. 5, p. 821.
2. Reed, T.B., *J. Appl. Phys.*, 1961, vol. 32, no. 12, p. 2534.
3. Kalinnikov, V.T. and Gutsol, A.F., *Dokl. Ross. Akad. Nauk*, 1997, vol. 353, no. 4, p. 469.
4. Gutsol, A.F. and Kalinnikov, V.T., *Teplofiz. Vys. Temp.*, 1999, vol. 37, no. 2, p. 194 (*High Temp.* (Engl. transl.), vol. 37, no. 2, p. 172).
5. Reed, T.B., *J. Appl. Phys.*, 1963, vol. 34, no. 8, p. 3146.
6. Dresvin, S.V., *Osnovy teorii i rascheta vysokochastotnykh plazmotronov* (The Fundamentals of Theory and Analysis of Radio-Frequency Plasmatrons), Leningrad: Energoatomizdat, 1991.
7. Boulos, M.I., *IEEE Trans. Plasma Sci.*, 1976, vol. PS-4, no. 1, p. 28.
8. Gutsol, A.F., Investigation and Optimization of Heat and Mass Transfer in Process Plasma Flows, *Doctoral (Tech.) Dissertation*, Moscow: IKhTREMS, 2000.
9. McKelliget, J.W. and El-Kaddah, N., *J. Appl. Phys.*, 1988, vol. 64, no. 6, p. 2948.
10. Mostaghimi, J. and Boulos, M.I., *Plasma Chem. Plasma Proc.*, 1989, vol. 9, no. 1, p. 25.
11. Chen Xi and Pfender, E., *Plasma Chem. Plasma Proc.*, 1991, vol. 11, no. 1, p. 103.
12. Chen, K. and Boulos, M.I., A Turbulent Flow Model of the R.F. Inductively Coupled Plasma, *Proc. 11th Int. Symp. on Plasma Chemistry*, England, 1993, vol. 1, p. 263.
13. Chen, K. and Boulos, M.I., *J. Phys. D*, 1994, vol. 27, p. 946.
14. Merkhouf, A. and Boulos, M.I., Experimental Validation for an Integrated Model of the Induction Plasma Generation System, *Proc. 14th Int. Symp. on Plasma Chemistry*, Prague, 1999, vol. 1, p. 421.
15. El-Hage, M., Mostaghimi, J., and Boulos, M.I., *J. Appl. Phys.*, 1989, vol. 65, no. 11, p. 4178.
16. Or, T., Subramanian, N.S., Heberlein, J., and Pfender, E., Analytical Studies of High Pressure, High Frequency (R.F.). Oxygen Plasmas, *Proc. 13th Int. Symp. on Plasma Chemistry*, Beijing, 1997, vol. 1, p. 380.
17. Ye, R., Proulx, P., and Boulos, M., Investigation of Turbulence Phenomena in the RF Plasma Torch, *Proc. 14th Int. Symp. on Plasma Chemistry*, Prague, 1999, vol. 1, p. 251.
18. Lesinski, J. and Boulos, M.I., *Plasma Chem. Plasma Proc.*, 1988, vol. 8, no. 2, p. 133.
19. Mostaghimi, J., Proulx, P., and Boulos, M.I., *J. Appl. Phys.*, 1987, vol. 61, no. 5, p. 1753.
20. Raizer, Yu.P., *Usp. Fiz. Nauk*, 1969, vol. 99, issue 4, p. 687.
21. Dymshits, B.M. and Koretskii, Ya.P., *Zh. Tekh. Fiz.*, 1969, vol. 39, no. 6, p. 1040.
22. Chase, D., *J. Appl. Phys.*, 1971, vol. 42, no. 12, p. 4870.
23. Dresvin, S.V. and El'-Mikati, Kh., *Teplofiz. Vys. Temp.*, 1977, vol. 15, no. 6, p. 1158.
24. Gutsol, A.F., Numerical Simulation of Reverse-Flow Swirl and Direct-Flow Swirl Heat Insulation of Plasma, *Trudy 2i Rossiiskoi natsional'noi konferentsii po teploobmenu* (Proc. 2nd Russian Nat. Conf. on Heat and Mass Transfer), Moscow: MEI (Moscow Inst. of Power Engineering—Educational), 1998, vol. 2, p. 104.
25. Hernberg, R.G., Jaffe, S.M., Larjo, J., *et al.*, Kinetic Gas and Electron Temperature Measurement in RF Induction

Plasma, *Proc. 10th Int. Symp. on Plasma Chemistry*, Germany, 1991, vol. 1, p. 1.2.

26. Gutsol, A., Larjo, J., and Hernberg, R., The Effect of Turbulence Model on the Simulation of Gas Flow in ICP, *Proc. 14th Int. Symp. on Plasma Chemistry*, Prague, 1999, vol. 1, p. 275.

27. Morvan, D., Erin, J., Magnaval, S., *et al.*, RF Multiflux Plasmatron Study. Experimental Measurements and Modeling, *Proc. 12th Int. Symp. on Plasma Chemistry*, Minnesota, 1995, vol. 3, p. 1743.

28. Owano, T.G., Gordon, M.H., and Kruger, C.H., *Phys. Fluids B*, 1990, vol. 2, no. 2, p. 3184.

29. Gupta, A.K., Lilley, D.G, and Syred, N., *Swirl Flows*, Abacus Press, 1984. Translated under the title *Zakruchennye potoki*, Moscow: Mir, 1987.

30. Hollenstein, M., Rahmane, M., and Boulos, M.I., Aerodynamic Study of the Supersonic Induction Plasma Jet, *Proc. 14th Int. Symp. on Plasma Chemistry*, Prague, 1999, vol. 1, p. 257.

31. Gutsol, A.F., *Usp. Fiz. Nauk*, 1997, vol. 167, no. 6, p. 665.

32. Abramovich, G.N. and Trofimov, R.S., *Inzh. Fiz. Zh.*, 1987, vol. 53, no. 5, p. 751.

33. Fin'ko, V.E., *Zh. Tekh. Fiz.*, 1983, vol. 53, issue 9, p. 1770.